Research on Chemical Intermediates (2022) 48:541–553
https://doi.org/10.1007/s11164-021-04631-3

A comparative study on dark adsorption of dyes using mesoporous MCM-41 catalyst

Rahmiye Zerrin Yarbay Şahin[1,2]

Received: 30 September 2021 / Accepted: 16 November 2021 / Published online: 24 November 2021

Abstract

Mobil composition of matter N. 41 (MCM-41) was investigated as a catalyst for the adsorption of methyl orange (MO) and setazol black (SB) under dark conditions. The MCM-41 catalyst was prepared via modified sol–gel method and fresh and spent catalysts were characterized by X-ray diffraction, scanning electron microscope, and Fourier-transform infrared spectroscopy. To examine the optimum conditions of dye adsorption, the catalyst dosage (0.2–1 g/L), contact time (5–240 min), and dye concentration (10–100 mg/L) were identified. The best performance showed that over 99.5% of methyl orange was removed in 60 min (concentration of dye = 20 mg/L, adsorbent dosage = 0.2 g/L, temperature = 22 °C). In case of SB, MCM-41 catalyst removed SB up to 95% under 60 min in 20 mg/L dye concentration. The MCM-41 catalyst was found to be more effective in removing MO through rather than SB with the help of the generation of reactive oxygen species. The spent catalysts characterization results concluded that the dark adsorption did not affect and announce a serious disorder on the pore structure of MCM-4. Consequently, the prepared MCM-41 presented a high catalytic efficiency and can be used especially for textile industry wastewater treatment applications at dark atmosphere in an energy-saving profile with no need of light irradiation.

Keywords Dark adsorption · Dye removal · MCM-41 · Methyl orange · Setazol black

✉ Rahmiye Zerrin Yarbay Şahin
zerrinyarbay@gmail.com; zerrin.yarbay@bilecik.edu.tr

[1] Chemical Engineering Department, Bilecik Seyh Edebali University, 11210 Bilecik, Turkey

[2] Energy Technologies Application and Research Centre, Bilecik Şeyh Edebali University, 11210 Bilecik, Turkey

Introduction

The environmental crisis has reached extraordinary proportions across the globe, acting major challenge for the biosphere [1]. As an important part of the environmental crisis, access to clean water and sanitation is reported as one of the Sustainable Development Goals accepted by the United Nations in 2015. Furthermore, it is reported that over two billion people in countries are suffering from high water stress circumstances. This drawback is a result of overuse of water resources with important influences on their sustainability [2]. The common pollutants in water resources can be listed as antibiotics [3], dyes [4], and heavy metals [5]. Anthropogenic activities resourcing from textile industry have environmental exposure risks and threats to living organisms in the water bodies and human health due to their discharge effluents include toxic components [6]. The textile industry is the leading industry branch in Turkey, covering 20% of the total industry. Besides, Turkey is one of the largest clothing suppliers in the European Union, ranking first in textiles, second in apparel, and seventh in the world [7]. Therefore, one of the most important classes of pollutants can be accepted as dyes. In case of existing in water, dye's synthetic character and complex molecular structure convert them to more stable and harder biodegradable pollutants [8]. It is of great interest to investigate the dye adsorption under dark conditions, especially room temperature and atmosphere pressure lacking additional lights or chemical stimulants [9].

To date, MCM-41 type mesoporous materials were utilized as substitute candidates for dye removal and metal removal in water depollution [10–24]. For example, Lee et al. [10] reported MCM-41 as a successful candidate for the removal of some basic dyes like rhodamine B (RB), crystal violet (CV), and methylene green (MG) from water solution which results no disorder on the pore structure. Juang et al. [16] pinpointed the possible effects of interaction between large dye molecules and concluded MCM-41 as a good catalyst for the removal of basic dyes. Qin et al. presented that ammonium-functionalized MCM-41 had a high affinity to four anionic dyes like methyl orange (MO), orange IV (OIV), reactive brilliant red X-3B (X-3B), and acid fuchsine (AF). They also claimed that while the amount of dye uptake was found to increase with the increase of contact time, the equilibrium time was independent of initial dye concentration [15]. Alardhi et al. [19] reported that MCM-41 was used for the first time as an efficient adsorbent to remove MG dye pollutants from synthetic wastewater in a fixed-bed column. Rios et al. found that when MCM-41 catalyst was examined for basic blue 41, methylene blue, basic red 18, and reactive red 239 dye, the catalyst was able to adsorb cationic compounds due to its surface chemistry. Therefore, they explored that their catalyst could not adsorb the reactive red 239 dye because of the negatively charged surface's adsorbing capability of cationic dyes through electrostatic interactions [24].

Previous studies demonstrated that MCM-41 dye removal efficiencies can be improved by metal doping or modifying using some reagents like silica tungstic acid (STA) [25], however, there are only a few studies focusing on improving the

efficiency of metal undoped MCM-41 [10–12, 16, 18–20, 24]. On the other hand, to the best of our knowledge, no studies have evaluated the removal of dye from the surface of MCM-41 in a dark ambient according to the literature. Therefore, this study examined the treatability of wastewaters with the dark ambient method with presence of a metal undoped mesoporous catalyst for the first time. In the experiments conducted with two different dye materials as MO and setazol black (SB), it was firstly aimed to determine the parameters effect on the treatment process used. With this way, besides searching dye concentration, catalyst dosage, and reaction duration influence, the efficiency of the dark dye removal was examined not only in the absence of metal doping to MCM-41 catalyst but also in a green and energy-saving way under dark conditions without adding any reducing and oxidizing agent or energy/light irradiation.

Materials and methods

Materials

Cetyltrimethylammonium bromide (CTAB; > 99%, $C_{16}H_{33}(CH_3)_3B$), ammonia (33%, Merck), and tetraethoxysilane (TEOS; > 98%, $Si(OC_2H_5)_4$, Aldrich) were used as received. Other reagents were of analytical grade from the suppliers. Distilled water was used in all solution preparations.

Two typical dyes, namely methyl orange and setazol black were chosen for the adsorption test in the dark at room temperature. SB which was produced by Setaş Kimya (Turkey) were used as received without further purification. Molecular weight of SB is 991.82 g/mol [26]. The chemical structure of this reactive diazo dye is given in Fig. 1 [27].

MO which was produced by Sigma-Aldrich is used without further purification in the experiments. MO is known as an acidic anionic mono-azo dye commonly and continuously used in textiles, laboratory experiments, and other commercial products [28]. MO has two chemical structures, whose chromophores are anthraquinone or azo bond depending on the pH of the solution, as can be expressed as [29] (Fig. 2).

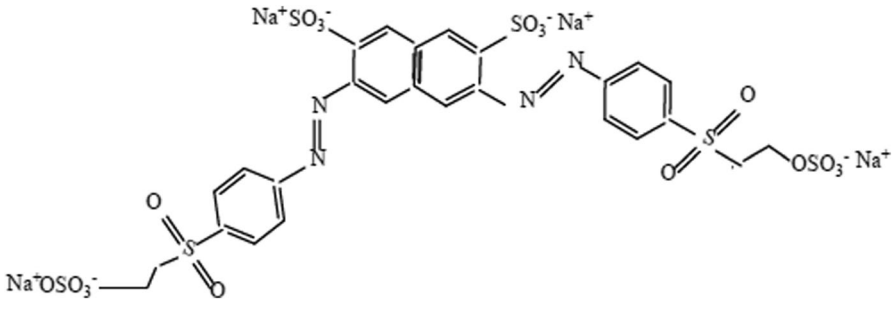

Fig. 1 Chemical structure of setazol black dye [24]

Fig. 2 Chemical structure of methyl orange dye [29–31]

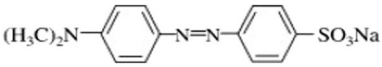

Catalyst preparation

In the literature, many different routes were successfully applied to prepare mesoporous MCM-41 material [10–24]. Although this material is commonly prepared by hydrothermal method [25], new approaches are developed [32]. Even though the sol–gel method is a very well-established method for catalyst preparation, the improvements of this method are shown to be applied in mesoporous materials in last years. Therefore, mesoporous MCM-41 was synthesized according to the recipe published by Yarbay Şahin, 2021 [32]. The details of the recipe are given in Fig. 3.

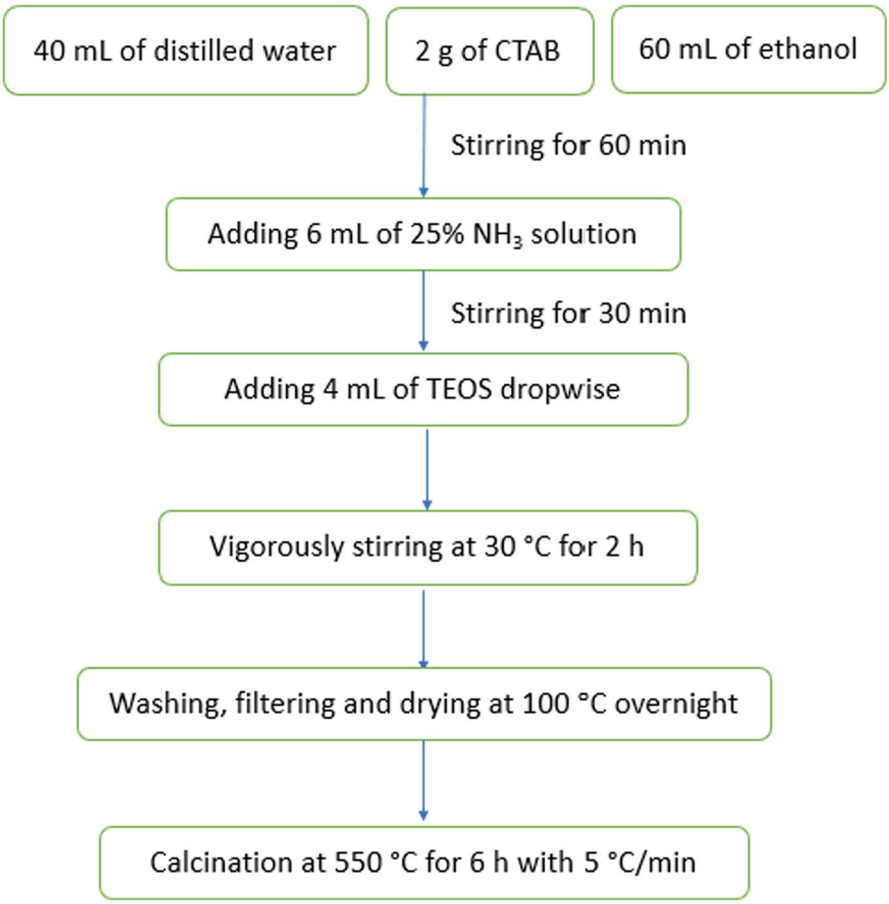

Fig. 3 Flow chart of the synthesis of MCM-41 using sol–gel method

Characterization

Preliminary investigations related to MCM-41 preparation via sol–gel method are done by our group and published in the reference given [32]. The BET results can be found in that article. Other characterization methods, including SEM, XRD, and FT-IR, were carried out in detail during this work. SEM micrographs of the fresh and spent catalysts were attained in Zeiss Supra VP 40. Phase identification of the fresh and spent catalysts was carried by Panalytical Empyrean diffractometer at 40 kV under Ni-filtered CuKα radiation ($\lambda = 0.15418$ nm). In the spectral range of 2100–600 cm^{-1}, FTIR analysis through Agilent Cary 630 Spectrometer was obtained for the fresh and spent catalysts.

Dye adsorption experiments

Dark adsorption experiments were implemented in order to investigate the effects of catalyst dosage (0.2–1 g/L), initial dye concentration (10–100 mg/L), and contact time (5–240 min). In order to prepare the stock solution, 1 g of MO and 1 g of SB were dissolved in 1 L of distilled water separately in order to reach a 1000 mg/L. Then, the adsorption tests were done by adding the desired amounts of MCM-41 to 50 mL of dye solution placed in 50 ml centrifuge tubes covered with aluminum foil at solution pH. All experiments were carried with continuous magnetic stirring in the dark at 22 °C. After the end of each run at designated intervals, suspensions were centrifuged at 7000 rpm for 10 min, filtered, and then the filtrate was collected for residual dye concentration measurement. Finally, the concentrations of dyes were determined at a maximum wavelength of MO (465 nm) and SB (596 nm) in ultraviolet–visible (UV–Vis) absorption spectra using a spectrophotometer (Agilent Cary 60). The concentrations of each dye before and after adsorption were determined from the standard calibration curve ($R^2 > 0.95$). Calculations after adsorption experiments were performed using the OriginPro 9.0 software. Each experiment was repeated two times. The adsorption efficiency (DE) of the dye was defined as follows in Eq. (1):

$$\mathrm{DE}(\%) = \frac{C_0 - C_t}{C_0} \times 100 \tag{1}$$

where C_0 is the initial concentration of the dye and C_t is the concentration at several reaction times (min).

The adsorbed amount per gram of MCM-41 (mg/g) or the adsorption capacity (q_e), was calculated using the following Eq. (2):

$$q_e = \frac{(C_i - C_f)V}{M} \tag{2}$$

where q_e is the adsorption capacity at equilibrium (mg/g), C_i and C_f (mg/L) are the initial and final concentrations, respectively, V (L) is the solution volume, and M (g) is the amount of MCM-41 used [11].

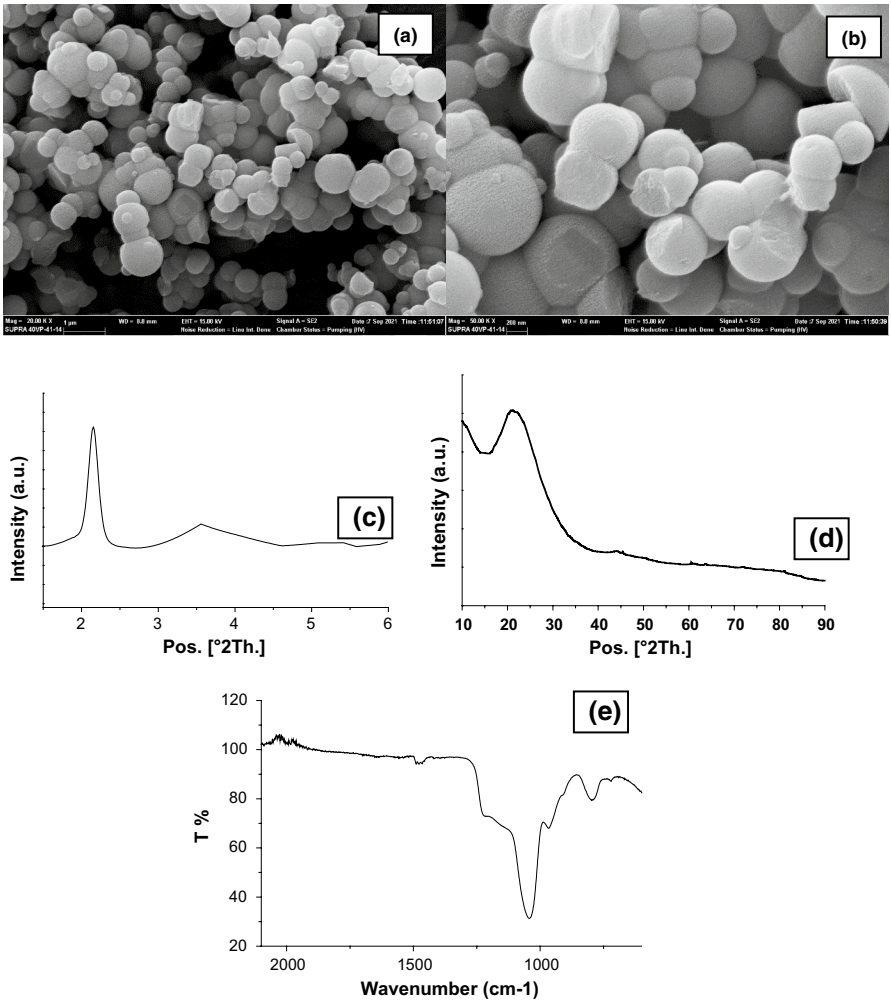

Fig. 4 SEM images of MCM-41 at **a** ×20,000, and **b** ×50,000 magnifications, XRD of MCM-41 **c** for low-angle measurement, and **d** for wide-angle measurement, **e** FT-IR of MCM-41

Results and discussion

Characterization of MCM-41

SEM, FTIR, and low-angle and wide-angle XRD results of the MCM-41 are shown in Fig. 4. SEM micrographs of the catalyst presented in Fig. 4a, b are spherical and elliptic nanoparticles. Similar achievements have been stated by Zhang et al. [14]. As shown in Fig. 4e FT-IR data, the absorption band at 1478 cm^{-1} corresponded to C-H vibrations of the surfactant molecules [33]. The Si–O–Si bands at 1037 and 783 cm^{-1} were attributed to asymmetrical and symmetrical stretching vibrations, respectively, and the band at about 560 cm^{-1} indicated the bending vibrations of the Si–O–Si groups. The absorption band at 437 cm^{-1} corresponds to the bending vibration of Si–O–Si. The small-angle XRD pattern given in Fig. 4c displayed a limited characteristic diffraction reflection for MCM-41. According to the results, a strong and sharp diffraction peak for $d(100)$ at 2.8 indicated a well-ordered lattice structure with hexagonal unit cell with JCPDS of 00-049-1712 [11, 34]. At a high-angle region (Fig. 4d), MCM-41 showed a broad peak ($2\theta = 23°$) ascribed to amorphous silica [35].

The Scherrer and the Williamson–Hall (W–H) equations were used to estimate the crystallite size for the MCM-41 sample. The Scherer equation is useful for the estimation of the samples with a grain size below 100 nm [36]. The MCM-41 particle diameter was estimated with Scherrer's equation [5] using the line-width at half-maximum of the X-ray diffraction peak at $2\theta = 2.15141$ with (100) reflection on XRD pattern was found as 52.58 nm. On the other hand, the W–H equation can evaluate the effects of both the crystallite size and lattice strain on the peak broadening simultaneously. This ability causes the wide application of this equation for the estimation of the size of crystals [37]. From the intercept of the W–H plot, a crystalline size of 68.64 nm was estimated for the composite. Therefore, it can be concluded that the closed size values confirmed that there is no strain effect, and thus, the results obtained by the Scherrer and Williamson–Hall equations are nearly equal [36].

Adsorption results

Dark adsorption is known as a new feasible alternative that discharges the necessity for light, and dissimilar other dark oxidation techniques with the help of not demanding supplementary chemicals (O_3, H_2O_2, SO_4) neither pH nor temperature regulations to run efficiently [33]. In the current dark adsorption experiments, the effects of catalyst dosage, initial dye concentration, and contact time were examined. All the experiments were studied at solution pH. The chemical characteristics of both adsorbent and adsorbate may differ with the pH value. The pH of the solution influences the degree of ionization and speciation of various dyes which subsequently primes to a variation in the reaction kinetics and equilibrium characteristics of the adsorption [8]. The pH of our pre-treatment solution without any

additives was measured as 6. In the literature, some investigations were carried at pH unchanged. Alardhi et al. studied "Adsorption of Methyl Green dye onto MCM-41" and their results indicated that when pH is higher than 8, the color of the solution turns from blue to approximately colorless, even with the absence of sorbent. Monash and Pugazhenthi measured the point of zero charge (PZC) of MCM-41 calcined at 550 C as 4.87. They stated that the favorable adsorption of a dye on MCM-41 can only take place when the solution pH is greater than pHpzc. Therefore, as a result, at higher pH (4–11), the pH of the solution is higher than pHpzc of the MCM-41 (4.87), which generally favors the adsorption of dye on MCM-41. The increased adsorption at higher pH (greater than pHpzc) is mainly related to the electrostatic attraction force of the dye compound with MCM-41 [20]. From the point of view of Methyl orange dye, Abo El Naga et al. studied about "Metal–organic framework-derived nitrogen-doped nanoporous carbon as an efficient adsorbent for methyl orange removal from aqueous solution". They reported that the pKa value of MO was 3.76 [38]. As a result, below pH 4.0 (lower than the pKa value of MO), MO anions would be protonated and thus positively charged. The electrostatic repulsion between the positively charged adsorbent surface and the protonated dye molecules may account for the low percentage of MO removal. At pH range from 4 to 6 (higher than the pKa value of MO), MO would exist mostly in anionic form. Consequently, the high percentage of MO removal in this pH range can be attributed to the strong electrostatic force of attraction between the positively charged adsorbent surface and the negatively charged dye molecules. Subsequent increase of solution pH makes the adsorbent surface negatively charged, and electrostatic repulsion exists between MO anions and adsorbent (in our study MCM-41), resulting in the decrease in the percentage of MO removal. In addition, the lower percentage of MO removal in basic environment was also ascribed to the competition between MO anions and the hydroxyl ions (OH^-) for the binding sites on the surface of the adsorbent. These results gave them an idea about evidence that the electrostatic interaction could be the main driving force governing the current adsorption process. Consequently, they carried out their experiments at a pH value of 6 [38]. Consequently, the pH was kept unchanged for subsequent experiments in their experiments.

For all dyes, the adsorption percentage tendency was recorded quite similarly as shown in Fig. 5a–c. This behavior of the catalyst highlights that the catalyst possesses high removal performance in all types of dyes. The high effectiveness for MCM-41 is ascribed to the higher accessibility of pores for the adsorption of dye molecules as possessing greater surface-active sites with high electrostatic attraction.

Catalyst dosage is an important factor to evaluate the adsorption activity of the catalyst [39]. Effect of catalyst dosage on MO and SB adsorption is shown in Fig. 5a. Both dyes displayed similar uptake values. It can be observed that as the catalyst dosage increased up to 0.2 g/L, the removal effectiveness improved to 75% and 87% for MO and SB, respectively. Indeed, SB displayed the maximum removal with 0.02 g catalyst as 79% which is quite similar to the 0.2 g/L catalyst used in experiment uptake. These results highlighted that any noteworthy improvement in dye removal was recorded using more than 0.2 g/L of the adsorbent dosage where the molecules are clustered into active sites which diminish MCM-41

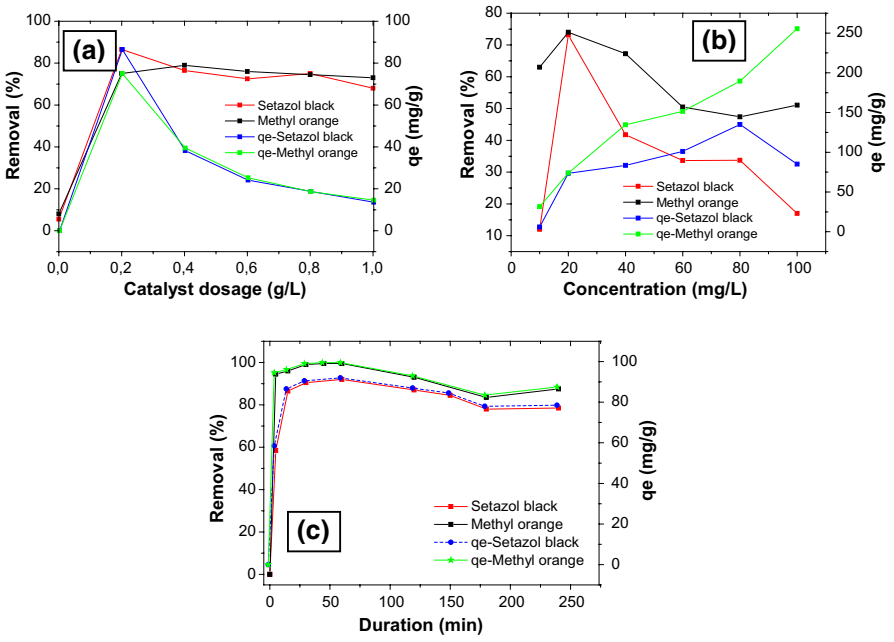

Fig. 5 Effect of **a** catalyst dosage (concentration of dye = 20 mg/L, contact time = 60 min, pH = 6, temperature = 22 °C), **b** dye concentration (catalyst dosage = 0.2 g/L, contact time = 60 min, pH = 6, temperature = 22 °C), and **c** contact time (concentration of dye = 20 mg/L, catalyst dosage = 0.2 g/L, pH = 6, temperature = 22 °C) on dye removal

available surface area [11]. As the adsorbent amount increased from 0.2 to 1 g/L, the adsorption capacities decreased from ≈ 87 mg/g for SB and 75 mg/g for MO to both ≈ 14 mg/g. This tendency could be understood in view of the surface area increment and the availability of more free adsorption sites, while the reduction in the adsorption capacities could be clarified bearing in mind that some of the adsorption sites endured unsaturated during the adsorption [40]. Therefore, the catalyst content at 0.2 g/L is optimum for the MCM-41 catalyst to remove MO and SB dyes, and all the reactions were performed using the above-optimized condition.

Dye concentration is an important indicator to estimate the activity of the catalysts for the adsorption of the organic dye [39]. Figure 5b presents the effect of dye concentration on the dark adsorption of MO and SB dyes of the MCM-41 catalyst. The adsorption percentage of the MCM-41 catalyst was highly dependent on the dye concentration. It is clear that the adsorption percentage decreases with the increasing the dye concentration for the dye concentration < 20 mg/L. The reason can be due to an increase in the driving force of the concentration gradient as the initial concentration increases [11]. On the other hand, the adsorption capacity of the MCM-41 was improved by increasing the dye concentration for both dyes. The result indicates that the dye concentration at about 20 mg/L is optimum for the MCM-41 catalyst to degrade both dyes [39].

The results obtained by investigating the effect of contact time/duration on the adsorption of the dyes are shown in Fig. 5c. The results indicated that the adsorption

rate was comparatively high at the beginning of the experiment which can be ascribed to the availability of active sites for dye adsorption, the previously mentioned binding sites turn out to be limited as the time runs [11]. The adsorption rate of the dyes was very fast achieving an amount above 90% which indicates that the dyes are not very stable in the dark in the presence of MCM-41 catalyst. After the initial 60 min of reaction, the MO dye was removed by 99.6% meanwhile SB was decomposed by 92%. The adsorption rate becomes slower with time as a result of the equilibrium state arises after 60 min, followed by an almost plateau up until the end of the experiment.

Characterization of the spent catalysts

The catalysts used in SB, and MO adsorption were characterized with XRD, SEM, and FT-IR techniques. The XRD patterns of the spent catalysts are demonstrated in Fig. 6a, b. The presence of *d*(100) diffraction peak in the fresh MCM-41 is an indication of good crystallinity but a slight change of the phase structure appears after adsorbing dyes. This change is recorded in only phase intensities. The XRD patterns of dye adsorbed catalysts showed much wider d(100) values than the corresponding peak observed for fresh MCM-41. The wide band corresponds to a wide distribution of pore sizes [33]. On the other hand, there is no sharp decrease in the intensity of MCM-41 peaks consequently there is no disorder in the pore structure of MCM- 41 which is consistent with FT-IR results.

The SEM images of MCM-41 after dye adsorption are shown in Fig. 5. When fresh (Fig. 4a, b) and spent catalysts (Fig. 6c–f) SEM images were compared, the mesoporous structure of fresh MCM-41 and spent MCM-41s can be clearly seen. Same crystals were observed before and after the dye adsorption. Particle size was also unchanged. The morphology investigations indicate that the morphology of MCM-41 is not demolished after dye adsorption. Dye adsorption made no visible difference to the particle morphology.

The FT-IR data in Fig. 6g show that dye adsorption made no visible difference to the catalyst structure. Furthermore, all characteristic peaks of fresh catalyst were detected for all spent samples, signifying the modification in the pore structure of MCM-41 encouraged by the dye's adsorption is more likely owing to the inherent disorder but not the collapse of the MCM-41 mesoporous structure [10]. Therefore, it can be stated that dye adsorption on the catalyst surface was insignificant during the adsorption [41].

Conclusion

A careful investigation about the removal of MO, and SB dyes by MCM-41 mesoporous catalyst is presented during this work. MCM-41 catalyst was synthesized by the sol–gel method. This catalyst was confirmed to be effective in the adsorption of the pollutants MO, and SB, under dark conditions without adding any reducing and oxidizing agent or energy/light irradiation. The catalyst shows

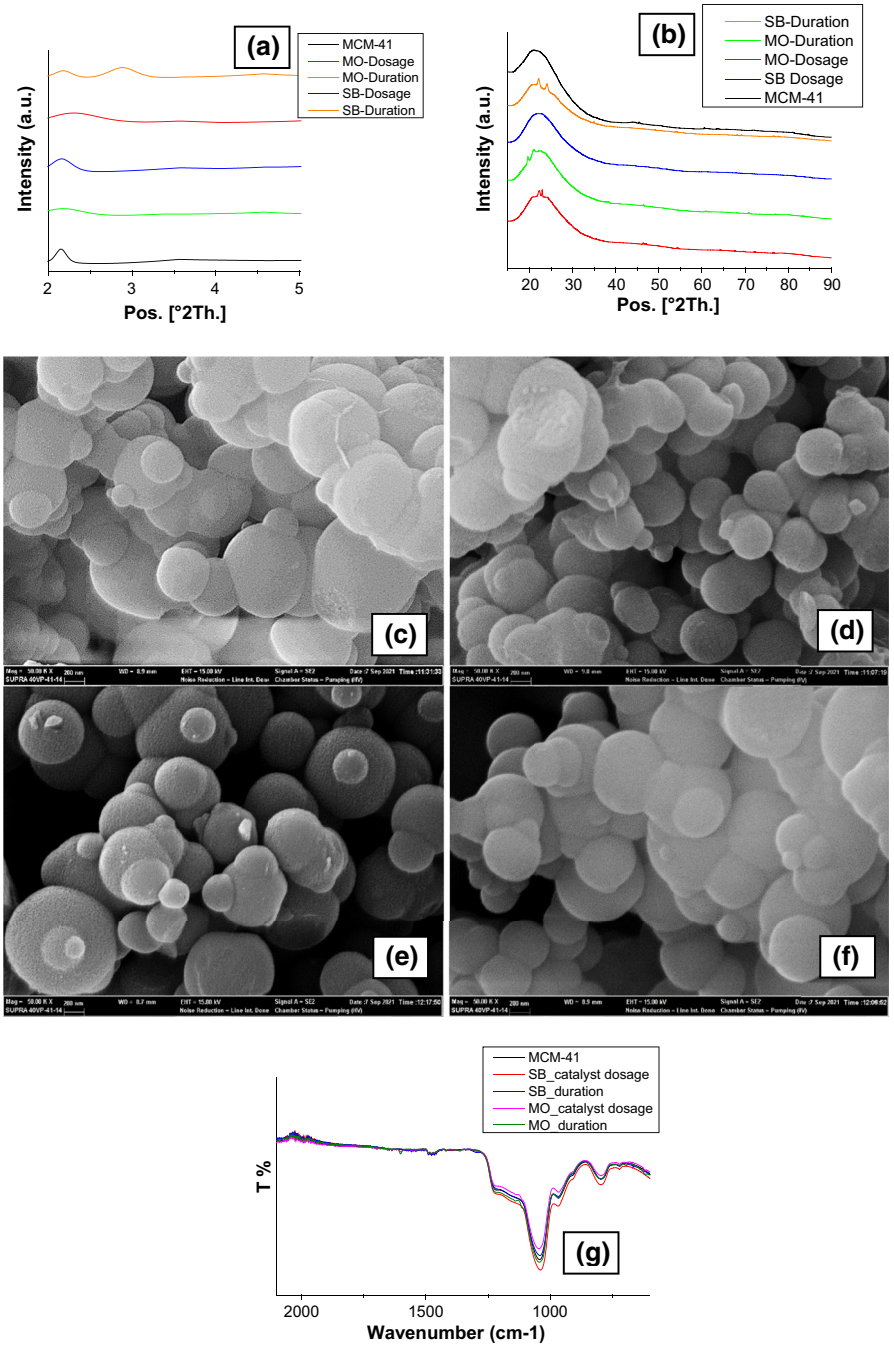

Fig. 6 XRD of spent MCM-41s **a** for low-angle measurement, and **b** for wide-angle measurement and SEM of the MCM-41 catalyst used in SB catalyst dosage experiment **c** ×50,000 magnification, used in SB duration experiment, **d** ×50,000 magnification, in MO catalyst dosage experiment, **e** ×50,000magnification, in MO duration experiment, **f** ×50,000 magnification and **g** FTIR spectra of spent MCM-41s

high removal performance in both types of dyes. The high removal performance is ascribed to the higher availability of pores for the adsorption of dye molecules with its larger surface-active sites. Notably, the MCM-41 was more effective in the adsorption of MO when compared to SB removal, reaching an abatement of 99.6% for MO and 96% for SB for 20 mg/L dye concentration during 60 min reaction duration irrespective of the pH. The detailed characterization investigations including SEM, FT-IR, and XRD analysis which were carried out for both fresh and spent catalysts indicated that no disorder of the mesoporous characteristic was observed for the catalyst. No visible difference in the catalyst structure after dye adsorption highlights that the change in the pore structure of MCM-41 encouraged by the dye's adsorption is more likely because of the inherent disorder but not the collapse of the MCM-41 mesoporous structure. Therefore, the dye adsorption on MCM-41 surface was unimportant during the dark adsorption. According to the results, it is easy to remove both dyes used in this study under dark conditions with higher levels of removal. This study highlights that the removal of dyes using MCM-41 prepared by sol–gel method is an extremely desirable energy-saving and efficient process that might find applications in dealing with environmental pollution.

Acknowledgements The author thanks to Dr. Nevin Atalay Gengeç and Assoc. Prof. Dr. Erhan Gengeç for their support during the centrifuge operation step.

Funding This research did not receive any specific grant from funding agencies in the public, commercial, or not-for-profit sectors.

Data availability The data that support the findings of this study are available from the corresponding author, RZYS, upon reasonable request.

Declarations

Conflict of interest The authors declare that they have no known competing financial interests or personal relationships that could have appeared to influence the work reported in this paper.

References

1. D. Bedada, K. Angassa, A. Tiruneh, H. Kloos, J. Fito, Energy Ecol. Environ. **5**(3), 184 (2020)
2. R. Dias, D. Sousa, M. Bernardo, I. Matos, I. Fonseca, V.V. Cardoso, R.N. Carneiro, S. Silva, P. Fontes, M.A. Daam, R. Maurício, Molecules **26**(4), 1010 (2021)
3. S. Azimi, A. Nezamzadeh-Ejhieh, J. Mol. Catal. A Chem. **408**, 152 (2015)
4. A. Nezamzadeh-Ejhieh, M. Karimi-Shamsabadi, Chem. Eng. J. **228**, 631 (2013)
5. M. Anari-Anaraki, A. Nezamzadeh-Ejhieh, J. Colloid Interface Sci. **440**, 272 (2015)
6. A.A. Bayode, F.O. Agunbiade, M.O. Omorogie, R. Moodley, O. Bodede, E.I. Unuabonah, Environ. Sci. Pollut. Res. **27**, 9957 (2020)
7. M. Atabey, Balıkesir University MSc Dissertation in Environmental Engineering (2019).
8. M.S. Secula, I. Cretescu, B. Cagnon, L.R. Manea, C.S. Stan, I.G. Breaban, Materials **6**(7), 2723 (2013)
9. W. Zhong, T. Jiang, Y. Dang, J. He, S.Y. Chen, C.H. Kuo, D. Kriz, Y. Meng, A.G. Meguerdichian, S.L. Suib, Appl. Catal. A Gen. **549**, 302 (2018)
10. C.K. Lee, S.S. Liu, L.C. Juang, C.C. Wang, K.S. Lin, M.D. Lyu, J. Hazard. Mater. **147**(3), 997 (2007)
11. S.M. Alardhi, J.M. Alrubaye, T.M. Albayati, Desalin. Water Treat. **179**, 323 (2020)

12. M.S. Yılmaz, Ö.D. Özdemir, S. Pişkin, Res. Chem. Intermed. **41**(1), 199 (2015)
13. G.E.D. Nascimento, M.M. Duarte, D.C. Sales, C.M.D.M. Barbosa, Chem. Eng. Commun. **204**(1), 105 (2017)
14. X. Zhang, J. Dong, Z. Hao, W. Cai, F. Wang, Trans. Tianjin Univ. **24**(4), 361 (2018)
15. Q. Qin, J. Ma, K. Liu, J. Hazard. Mater. **162**(1), 133 (2009)
16. L.C. Juang, C.C. Wang, C.K. Lee, Chemosphere **64**(11), 1920 (2006)
17. B. Boukoussa, R. Hamacha, A. Morsli, A. Bengueddach, Arab. J. Chem. **10**, 2160 (2017)
18. L.C. Juang, C.C. Wang, C.K. Lee, T.C. Hsu, J. Environ. Eng. Manag. **17**(1), 29 (2007)
19. S.M. Alardhi, T.M. Albayati, J.M. Alrubaye, Heliyon **6**(1), 03253 (2020)
20. P. Monash, G. Pugazhenthi, Korean J. Chem. Eng. **27**(4), 1184 (2010)
21. B. Nanda, A.C. Pradhan, K.M. Parida, Microporous Mesoporous Mater. **226**, 229 (2016)
22. Y. Shu, Y. Shao, X. Wei, X. Wang, Q. Sun, Q. Zhang, L. Li, Microporous Mesoporous Mater. **214**, 88 (2015)
23. Y. Shao, X. Wang, Y. Kang, Y. Shu, Q. Sun, L. Li, J. Colloid Interface Sci. **429**, 25 (2014)
24. A.G. Rios, L.C. Matos, Y.A. Manrique, J.M. Loureiro, A. Mendes, A.F. Ferreira, Adsorption **26**(1), 75 (2020)
25. V. Şimşek, K. Mürtezaoğlu, Bilecik Şeyh Edebali Üniversitesi Fen Bilimleri Dergisi **6**(1), 91 (2019)
26. S. Ledakowicz, L. Bilińska, Proceedings of ECOpole, vol. 6 (2012).
27. T. Öztürk, H. Akbaş, G.A. Keskin, MANAS J. Eng. **8**(2), 115 (2020)
28. A.A.A. Darwish, M. Rashad, H.A. Al-Aoh, Dyes Pigments **160**, 563 (2019)
29. Y. Yao, H. Bing, X. Feifei, C. Xiaofeng, Chem. Eng. J. **170**(1), 82 (2011)
30. S. Chen, J. Zhang, C. Zhang, Q. Yue, Y. Li, C. Li, Desalination **252**(1–3), 149 (2010)
31. Q. Yang, S. Ren, Q. Zhao, R. Lu, C. Hang, Z. Chen, H. Zheng, Chem. Eng. J. **333**, 49 (2018)
32. R.Z. Yarbay Şahin, J. Turk. Chem. Soc. Sect. B Chem. Eng. **4**(2), 27 (2021)
33. C. Huo, J. Ouyang, H. Yang, Sci. Rep. **4**(1), 1 (2014)
34. E.K. Ekinci, N. Oktar, Green Process. Synth. **8**(1), 128 (2019)
35. T. Sun, M. Gong, Y. Cai, S. Xiao, L. Zhang, Y. Zhang, Z. Xu, D. Zhang, Y. Liu, C. Zhou, Res. Chem. Intermed. **46**(1), 459 (2020)
36. N. Raeisi-Kheirabadi, A. Nezamzadeh-Ejhieh, Int. J. Hydrogen Energy **45**(58), 33381 (2020)
37. S. Ghattavi, A. Nezamzadeh-Ejhieh, J. Mol. Liquids **322**, 114563 (2021)
38. A.O.A. El Naga, S.A. Shaban, F.Y. El Kady, J. Taiwan Inst. Chem. Eng. **93**, 363 (2018)
39. Y. Wang, J. Song, Z. Phys. Chem. **234**(1), 153 (2020)
40. V. Rizzi, J. Gubitosa, P. Fini, S. Nuzzo, P. Cosma, Sustain. Mater. Technol. **26**, e00231 (2020)
41. H. Chen, J. Motuzas, W. Martens, J.C.D. da Costa, Sep. Purif. Technol. **205**, 293 (2018)